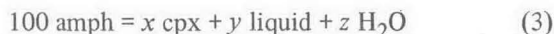Fig. 3. Amphibole stability in 1921 Kilauea tholeiite. Curve for $X^{fl}_{H_2O}$ = 0.6 from Holloway [3]. Brackets, with representations as in fig. 2, refer to H_2O-saturated runs at QFM buffer. Run at 5 kb by R. Tuthill (reported in [3]).
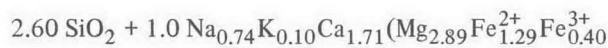
The reaction is written in weight percent. Recognizing that the H_2O-undersaturated liquid contains 4.7 percent H_2O at 5.0 kb, and that amphibole contains 2 percent H_2O, we may rewrite the reaction:
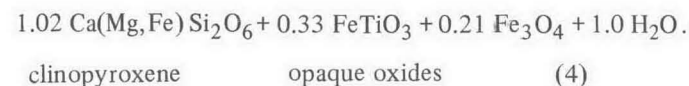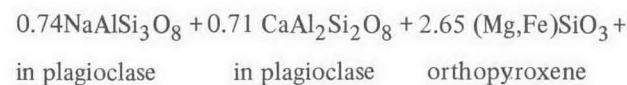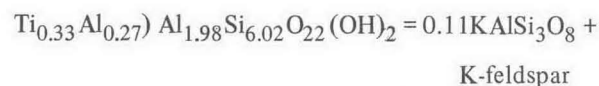
$$100 \text{ amph} + 1.6 \text{ } H_2O = 23 \text{ cpx} + 77 \text{ liquid} \qquad (2)$$

This equation predicts the increased stability of amphibole with decreased f_{H_2O}. However, experiments explained above show that as weight H_2O in melt is decreased below 4.5 percent at 5.5 kb, amphibole stability decreases, and that an isobaric maximum of stability exists. Since eq. (2) does not predict this behavior, another equation is needed. Two possibilities are a modification of (2),

$$100 \text{ amph} = x \text{ cpx} + y \text{ liquid} + z \text{ } H_2O \qquad (3)$$

and the subsolidus dehydration reaction:

$$2.60 \text{ } SiO_2 + 1.0 \text{ } Na_{0.74}K_{0.10}Ca_{1.71}(Mg_{2.89}Fe^{2+}_{1.29}Fe^{3+}_{0.40}$$

quartz   amphibole

$$Ti_{0.33}Al_{0.27})Al_{1.98}Si_{6.02}O_{22}(OH)_2 = 0.11KAlSi_3O_8 +$$

K-feldspar

$$0.74NaAlSi_3O_8 + 0.71 \text{ } CaAl_2Si_2O_8 + 2.65 \text{ } (Mg,Fe)SiO_3 +$$

in plagioclase   in plagioclase   orthopyroxene

$$1.02 \text{ } Ca(Mg,Fe)Si_2O_6 + 0.33 \text{ } FeTiO_3 + 0.21 \text{ } Fe_3O_4 + 1.0 \text{ } H_2O.$$

clinopyroxene   opaque oxides   (4)

The amphibole composition is that of analysis 2, table 1. At temperatures above the solidus, SiO_2 and $KAlSi_3O_8$ undoubtedly melt just above the solidus; the other breakdown products are solid phases, except plagioclase above 4.5 kb in H_2O-saturated melts.

Reaction (3) is possible if the 2.0 percent H_2O produced by amphibole breakdown is greater than the weight solubility of H_2O in the melt at the total pressure, temperature and $X^{fl}_{H_2O}$ of interest. Such a condition results when H_2O solubility in the melt decreases with decreased $X^{fl}_{H_2O}$ or when the amount of melt is decreased by an increased ratio of x to y. Assuming the coefficients of (3) at 5 kb hold in andesite melt at 5.5 kb, however, so that $x = 23$ and $y = 77$ (weight), a liquid containing 4.4 percent H_2O cannot be produced by melting 100 percent amphibole. It appears that z is negative for andesite melt containing 4.4 percent H_2O at 5.5 kb, and that eq. (3) is invalid.

Eq. (4) remains to explain the observed behavior. Because the solidus temperature approaches the temperature of the amphibole-out curve when $X^{fl}_{H_2O}$ is decreased (fig. 4), this reaction is intuitively reasonable. The calculations of fig. 4 show also that the reaction is thermodynamically reasonable. These calculations are based on the argument that amphibole will melt by reaction (2) only within its stability field, and that the amphibole-out reaction will change from melting to dehydration when the isobaric dehydration curve for any $X^{fl}_{H_2O}$ is lower in temperature than the metastable melting curve for the same $X^{fl}_{H_2O}$ and total pressure. It follows that at those isobaric points at which the reaction changes, the dehydration and melting curves for a particular $X^{fl}_{H_2O}$ must cross, because

at those points $f^m_{H_2O}$ calculated for the melting reaction is equal to $f^{fl}_{H_2O}$ calculated for the dehydration curve.

By the above reasoning, one point on the family of dehydration curves is known, 935°C at 5.5 kb for $X^{fl}_{H_2O} = 0.44$. Strictly speaking, dehydration at those conditions is not equivalent to dehydration of reaction (4), because SiO_2, $KAlSi_3O_8$, and, for H_2O contents in melt greater than 4.7 percent, the oxide phases are dissolved in the melt. However, only activity of SiO_2 is quantitatively significant in the equilibrium constant, and its activity in Paricutin melt, calculated from compositions of coexisting olivine and ortho-pyroxene in experimental runs and the thermochemical data of Williams [13], is nearly 1.0. Another point on the family of curves was assumed from the intersection of the H_2O-saturated amphibole-out curve and the solidus. From these two points and the molar volume change of the solid phases for reaction (4), the family of dehydration curves (fig. 4a) was constructed.

In fig. 4b the H_2O-saturated amphibole-out curve is assumed to be the melting reaction of eq. (2). Although the position of this curve for lower $X^{fl}_{H_2O}$ is not known, it must lie to the right of the H_2O-saturated position, as long as the melting reaction is (2), not (3).

Fig. 4c combines the curves of figs. 4a and 4b to produce amphibole-out curves which would be observed experimentally at various $X^{fl}_{H_2O}$. Although the curves are not claimed to be positionally correct quantitatively, their relative schematic position is probably correct. According to fig. 4c, for a $X^{fl}_{H_2O} = 1$, the observed amphibole-out curve is a melting reaction at all pressures above 900 bars, a pressure below which the dehydration curve for $X^{fl}_{H_2O} = 1$ marks the upper stability limit of amphibole. At a $X^{fl}_{H_2O} = 0.2$, the upper stability limit of amphibole is the dehydration reaction at all pressures. Therefore the amphibole melting curve for $X^{fl}_{H_2O} = 0.2$ in fig. 4b is metastable. For $X^{fl}_{H_2O} =$
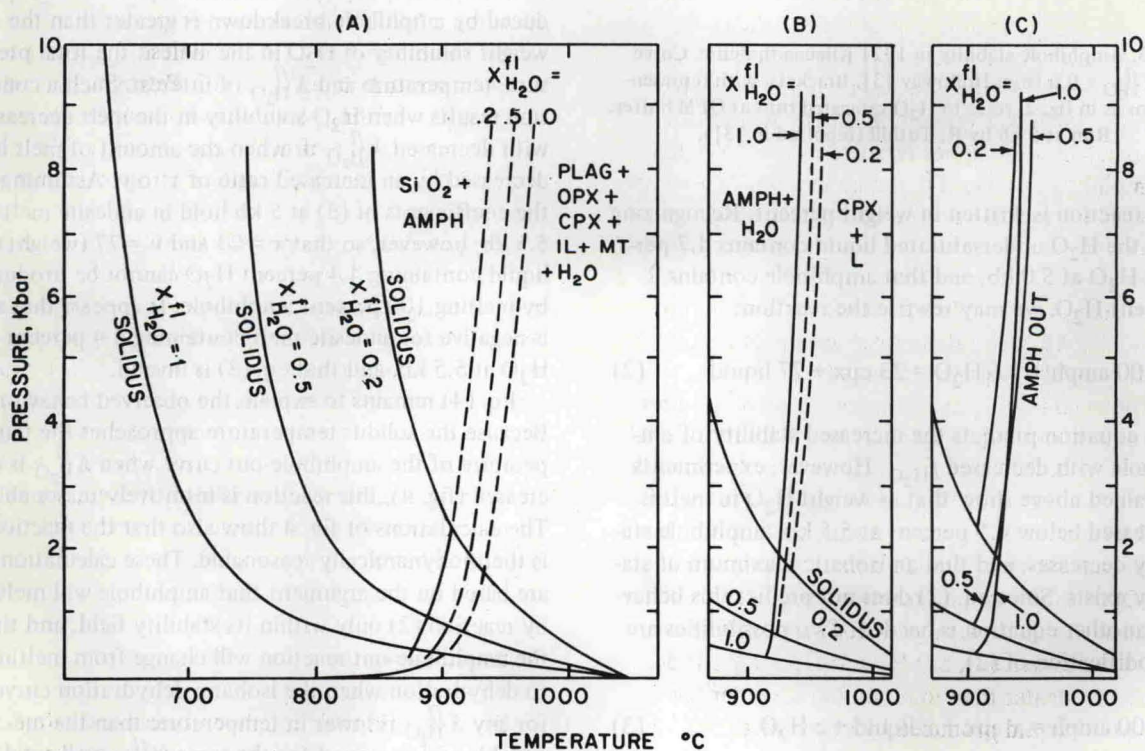

Fig. 4. Schematic P-T projection of solidus and amphibole-out reactions for various $X^{fl}_{H_2O}$. (a) Solidus for andesite-H_2O, after tonalite solidus of [14]; H_2O-undersaturated solidi, calculated from data of [15]; and amphibole + quartz dehydration curves, dashed where metastable. (b) Incongruent melting curves of amphibole in andesite melt for $X^{fl}_{H_2O} = 1.0$ (experimental) and 0.2 and 0.5 (dashed, may be metastable). (c) Upper stability limits of amphibole in andesite melt for various $X^{fl}_{H_2O}$.